Journal of Cosmetics, Dermatological Sciences and Applications, 2025, 15(3), 159-176
https://www.scirp.org/journal/jcdsa
ISSN Online: 2161-4512
ISSN Print: 2161-4105

Multi-Pathway Fibroblast Modulation by PDRN Restores Dermal Structure and Improves Periocular Aging

Suqing Liu[1], Qianqian Wang[1], Mingyu Wang[2,3], Chenqiong Yan[2,3], Rui Ye[2,3], Le Du[2,3], Fan Hu[2,3*]

[1]Department of Dermatology, Huashan Hospital, Fudan University, Shanghai, China
[2]UNISKIN Research Institute on Skin Aging, Inertia Shanghai Biotechnology Co., Ltd., Shanghai, China
[3]DermaHealth Shanghai Biotechnology Co., Ltd., Shanghai, China
Email: *hufan@uniskin.com

How to cite this paper: Liu, S.Q., Wang, Q.Q., Wang, M.Y., Yan, C.Q., Ye, R., Du, L. and Hu, F. (2025) Multi-Pathway Fibroblast Modulation by PDRN Restores Dermal Structure and Improves Periocular Aging. *Journal of Cosmetics, Dermatological Sciences and Applications*, **15**, 159-176.
https://doi.org/10.4236/jcdsa.2025.154010

Received: August 26, 2025
Accepted: October 24, 2025
Published: October 27, 2025

Abstract

Background: Polydeoxyribonucleotide (PDRN), a DNA-derived macromolecule, has demonstrated regenerative potential in dermatology, yet its molecular mechanisms in skin anti-aging remain underexplored. This study investigated the cellular and transcriptomic mechanisms of PDRN and validated its clinical efficacy in periocular rejuvenation. **Methods**: Human dermal fibroblasts (HDFs) were subjected to UVB-induced damage and treated with PDRN. Cell viability was evaluated by MTT assay, while immunohistochemistry (IHC) assessed type I/III collagen and elastin expression. Transcriptomic changes were profiled by RNA sequencing with pathway annotation through GO and KEGG analyses. *Ex vivo* Raman spectroscopy was used to characterize PDRN skin penetration. Finally, a randomized, double-blind, split-face clinical trial in 33 women compared the efficacy of a PDRN-containing eye cream with placebo after 28 days of use. **Results**: PDRN significantly restored collagen I/III and elastin expression in UVB-damaged fibroblasts. RNA-seq revealed a multi-pathway modulatory mechanism whereby PDRN: 1) activated PI3K-Akt and TGF-β signaling to promote ECM regeneration, 2) enhanced autophagy-lysosome and spliceosome activity to restore proteostasis, and 3) suppressed chemokine signaling to rebalance fibroblast-immune interactions. *Ex vivo* Raman spectroscopy confirmed that PDRN penetrates into the dermis. Clinically, a PDRN-containing eye cream significantly improved periocular elasticity and firmness, increased dermal density (+8.67%), reduced wrinkle number and volume, decreased under-eye bag volume (–18.42%), and enhanced skin brightness (+4.88%) compared with placebo (all $p < 0.05$). Morphometric analysis further demonstrated improvements in periocular contour geometry. **Conclusion**: PDRN exerts anti-aging effects through multi-path-

way modulation of fibroblast activity—integrating ECM repair, proteostasis, and immune modulation—establishing it as a clinically effective macromolecular active for periocular skin rejuvenation.

Keywords

Polydeoxyribonucleotide, Periocular Aging, Extracellular Matrix Regeneration, Multi-Pathway Modulation, RNA Sequencing

1. Introduction

Skin aging is a multifactorial biological process influenced by both intrinsic (chronological) and extrinsic (environmental) factors [1]. Intrinsic aging is genetically determined and manifests gradually with time, whereas extrinsic aging is predominantly driven by environmental stressors, among which ultraviolet (UV) radiation is the most potent inducer of photoaging [2] [3]. Chronic UV exposure accelerates skin aging by triggering oxidative stress, DNA damage, and persistent inflammatory responses, ultimately compromising the structural and functional integrity of the skin barrier [4].

At the cellular level, UV radiation impairs the viability and biosynthetic function of dermal fibroblasts, the principal stromal cells responsible for producing extracellular matrix (ECM) proteins such as collagen types I and III, elastin, and glycosaminoglycans (GAGs) [5]. UV irradiation also upregulates matrix metalloproteinases (MMPs), which degrade structural proteins and exacerbate ECM breakdown [6]. The resulting imbalance between ECM synthesis and degradation manifests clinically as wrinkles, dermal thinning, and loss of skin elasticity [7].

Current topical anti-aging interventions commonly employ retinoids, vitamin C derivatives, peptides, and antioxidants, which target pathways such as collagen synthesis, oxidative stress reduction, or epidermal renewal [8]-[11]. While effective in part, these agents often act on one or two biological mechanisms and may be limited by irritation, photosensitivity, or poor tolerability in sensitive skin [12] [13]. Thus, there is an unmet need for multifunctional actives capable of simultaneously addressing ECM degradation, cellular stress, and impaired regenerative capacity, particularly under UV-compromised conditions.

Polydeoxyribonucleotide (PDRN), a DNA-derived polymer extracted from the sperm of salmonid species, has emerged as a promising candidate for skin repair and rejuvenation. With an average molecular weight ranging from 50 to 1500 kDa, PDRN exerts pro-regenerative effects through activation of adenosine A2A receptors, stimulation of angiogenesis, and promotion of wound healing [14]. Clinically, PDRN has been utilized in chronic wound management, ischemic disease, and post-laser recovery [15] [16]. Preclinical evidence also suggests roles in ECM regeneration and inflammation modulation [17]. However, its precise mechanisms in the context of cutaneous aging remain incompletely understood.

A critical barrier to topical application of macromolecules such as PDRN is

their ability to traverse the stratum corneum and reach the dermis, where fibroblasts reside [18]. To date, few studies have directly evaluated the skin penetration of PDRN. In this work, we address this gap by performing *ex vivo* Raman spectroscopy to visualize and quantify the time-dependent diffusion of PDRN across human skin layers. Demonstrating that PDRN can reach both the epidermis and dermis provides essential translational evidence supporting its potential as a topical anti-aging agent.

In this study, we therefore aimed to comprehensively characterize the anti-aging mechanisms and benefits of PDRN using a tiered experimental design. First, we examined its effects on ECM protein expression—specifically collagen I, collagen III, and elastin—in UV-damaged human dermal fibroblasts through immunofluorescence staining. To elucidate the underlying molecular pathways, we performed RNA sequencing (RNA-seq) of PDRN-treated fibroblasts, focusing on signatures related to ECM remodeling, proteostasis, cell survival, and inflammation. We then evaluated PDRN penetration into *ex vivo* human skin using Raman spectroscopy, followed by a randomized controlled clinical trial of a PDRN-containing eye cream to assess improvements in visible signs of periorbital aging.

Together, these investigations provide the first mechanistic, penetration, and clinical evidence supporting PDRN as a multifunctional anti-aging agent, capable of engaging regenerative pathways, traversing the skin barrier, and improving clinical outcomes in UV-damaged skin.

2. Materials and Methods

2.1. Materials

PDRN used in this study was kindly provided by Ruijiming (Shandong) Biotechnology Co., Ltd. The material is a high-purity (≥96%) DNA polymer extracted from salmon sperm, with an average fragment length of approximately 1246.6 base pairs and an average molecular weight not exceeding 850 kDa. It was supplied in lyophilized powder form and reconstituted in sterile water or culture medium immediately prior to use.

2.2. MTT Assay

Human dermal fibroblasts (HDFs) were seeded in 96-well plates and allowed to attach overnight. At approximately 80% confluence, cells were treated with PDRN at concentrations ranging from 0.1 to 100 μg/mL for 48 h. Subsequently, 10 μL of MTT solution (5 mg/mL in PBS) was added to each well, followed by incubation at 37˚C for 4 h. The medium was then aspirated, and 100 μL of DMSO was added to dissolve the formazan crystals. Plates were gently agitated for 15 min to ensure complete solubilization, and absorbance was measured at 490 nm using a microplate reader (iD3, Molecular Devices, USA) to determine cell viability.

2.3. Cell Culture and UV Irradiation

Human dermal fibroblasts were cultured in Dulbecco's Modified Eagle Medium

(DMEM; CGM101.05, Cellmax, CHN) supplemented with 10% fetal bovine serum (FBS; 04-001-1ACS, BI, IL) and 1% penicillin-streptomycin (P1400, Solarbio, CHN). For immunofluorescence experiments, cells were seeded into 96-well glass-bottom plates and cultured to 70% - 80% confluence. Cells were then treated with PDRN at the indicated concentrations for 48 h. After treatment, the medium was removed, cells were rinsed with PBS, and exposed to UVB irradiation at 200 mJ/cm^2 (wavelength range 290 - 330 nm, peak 309.3 nm) using a calibrated UVB lamp, with irradiance monitored by a UV irradiance meter (HP250, Hangzhou LCE Intelligent, CHN). Non-irradiated controls were handled identically but shielded from UVB. Immediately following irradiation, PBS was replaced with serum- and antibiotic-free DMEM, and cells were incubated for an additional 48 h before fixation and immunostaining.

For RNA sequencing, UVB-irradiated HDFs were prepared under identical treatment conditions. After the post-irradiation incubation, total RNA was extracted for transcriptomic profiling.

2.4. Immunohistochemistry (IHC) Staining

Following UVB irradiation and post-treatment incubation, HDFs in 96-well glass-bottom plates were processed for immunofluorescence staining. Cells were gently washed twice with PBS and fixed with 4% paraformaldehyde (P1110, Solarbio, CHN) for 15 minutes at room temperature (RT). After fixation, cells were permeabilized with 0.1% Triton X-100 in PBS for 10 minutes, followed by PBS washes. Non-specific binding was blocked with 5% BSA blocking buffer (SW3015, Solarbio, CHN) for 1 hour at RT. Cells were then incubated with the following antibodies for fluorescence staining: Alexa Fluor® 488-conjugated anti-collagen I antibody (1:100, ab275996, Abcam, UK), incubated for 1 hour at RT; Alexa Fluor® 546-conjugated anti-elastin antibody (1:50, sc-58756 AF546, Santa Cruz Biotechnology, USA), incubated for 1 hour at RT; Anti-collagen III primary antibody (1:250, ab7778, Abcam, UK), incubated overnight at 4˚C, followed by Alexa Fluor® 488-conjugated goat anti-mouse IgG secondary antibody (1:500, A11008, Invitrogen, UK) for 1 hour at RT. Cell nuclei were counterstained with DAPI (C0065, Solarbio, CHN) for 5 minutes at RT, then washed with PBS. Fluorescence images were acquired using an inverted fluorescence microscope (Leica DMi8) equipped with a 20× objective.

2.5. RNA Sequencing (RNA-Seq) Analysis

Total RNA was extracted from UVB-irradiated and PDRN-treated HDFs using TRIzol Reagent (Invitrogen, USA). RNA integrity and concentration were assessed with an Agilent 2100 Bioanalyzer and Qubit Fluorometer, and only samples with RIN > 7.0 and 28S: 18S ratio > 1.8 were used for library preparation. RNA-seq libraries (biological triplicates per group) were prepared by CapitalBio Technology (Beijing, China). Poly(A) + mRNA was isolated from 1 μg of total RNA, fragmented (~200 bp), and reverse-transcribed to first-strand cDNA, followed by sec-

ond-strand synthesis. After end repair, A-tailing, and adapter ligation, libraries were amplified using the NEBNext Ultra RNA Library Prep Kit (NEB, USA), quality-checked with the KAPA Library Quantification Kit and Agilent 2100 Bioanalyzer, and sequenced on an Illumina NovaSeq 6000 platform (paired-end, 150 bp).

Raw sequencing reads were quality-checked with FastQC (v0.11.5) and filtered using the NGSQC Toolkit (v2.3.3). Clean reads were aligned to the human reference genome (GRCh38/hg38) using HISAT2 (v2.1.0), and transcripts were assembled and quantified with StringTie (v1.3.3b). Differential gene expression was analyzed using DESeq (v1.28.0), with significance thresholds set at $|\log_2 FC| \geq 1$ and $p \leq 0.05$, followed by Benjamini–Hochberg correction to obtain adjusted p-values. Functional annotation of differentially expressed genes (DEGs) was performed using ENSEMBL, NCBI, UniProt, Gene Ontology (GO), and Kyoto Encyclopedia of Genes and Genomes (KEGG) databases.

2.6. *Ex Vivo* Skin Penetration by Raman Spectroscopy

Ex vivo penetration of PDRN was evaluated using full-thickness human skin mounted in Franz diffusion cells, with the stratum corneum oriented toward the donor chamber and the dermal side in contact with PBS receptor medium. To yield a detectable and quantifiable Raman signal, an aqueous solution containing 0.025% PDRN (effective diffusion area ≈ 0.785 cm^2) was uniformly applied to the skin surface and maintained at 32˚C ± 1˚C under continuous magnetic stirring (300 rpm). Skin specimens were collected at 2, 6, and 24 h, rinsed to remove residual formulation, excised, and cryosectioned.

Confocal Raman spectroscopy, calibrated against a silicon wafer, was performed on cryosections mounted on quartz gold-coated slides, with intact regions of epidermis and dermis selected for analysis. Spectra were acquired at characteristic PDRN peaks, and Raman mapping was used to generate depth-resolved distribution profiles.

Spectral preprocessing (cosmic ray removal, baseline correction, smoothing) and chemical image reconstruction were performed using Witec Project software. The integrated intensity of PDRN-specific peaks was used to generate pseudocolor penetration maps. Origin software was employed for spectral plotting and semi-quantitative analysis, and statistical analysis was conducted using GraphPad Prism with a two-tailed t-test, with $p < 0.05$ considered significant.

2.7. Clinical Evaluation of PDRN Eye Cream

The clinical study was conducted at Hangzhou Sinotek Quality & Testing Services Co., Ltd. and approved by the Sinotek Ethics Committee for Clinical Research (project number SWPN250609). A total of 33 healthy women aged 35 - 55 years were enrolled. Inclusion criteria included sensitive skin (Huaxi Questionnaire ≥ 18) with symptoms such as burning or stinging upon irritation, and symmetrical periocular aging defined as crow's feet > grade 2, under-eye wrinkles > grade 2, and eye bags > grade 1 (Skin Age Atlas - Asian Type). Exclusion criteria comprised

dermatologic or systemic disease, pregnancy or lactation, periocular implants, wounds, infections, or other conditions likely to interfere with study outcomes. Written informed consent was obtained from all participants.

The study employed a randomized, double-blind, split-face design. In one cohort, a PDRN eye cream containing 100-fold the *in vitro* effective concentration of PDRN was applied to the left periocular area, and placebo to the right; in the other cohort, the assignment was reversed. This concentration (10 μg/mL) was selected based on the in vitro effective range (0.1 - 0.25 μg/mL) while accounting for the significant barrier posed by the stratum corneum, with a ~100-fold increase applied as a translational safety margin to ensure skin bioactivity while maintaining tolerability in a sensitive-skin cohort. After facial cleansing, a fixed dose was applied to the upper and lower eyelids, glabellar, and sub-brow regions, massaged until absorbed, twice daily for 28 days. Assessments were performed at baseline and day 28.

Standardized photography (EOS 700D, Canon) with Image-Pro Plus (IPP) analysis was used to measure periocular geometric parameters (angles A and B, distances L1 - L3, palpebral fissure area, and angle C; see Figure 1). Wrinkle number and area were evaluated using VISIA 7 (Canfield) with IPP, skin roughness (Sa) with Primos CR, tear trough length/volume and eye bag volume with Antera 3D, hydration with Corneometer CM825, gloss with Glossymeter GL200, brightness (L*) with Colorimeter CL400, elasticity parameters (R0, F4, R2, R5, R7) with Cutometer MPA580, and dermal density with Ultrascan UC22.

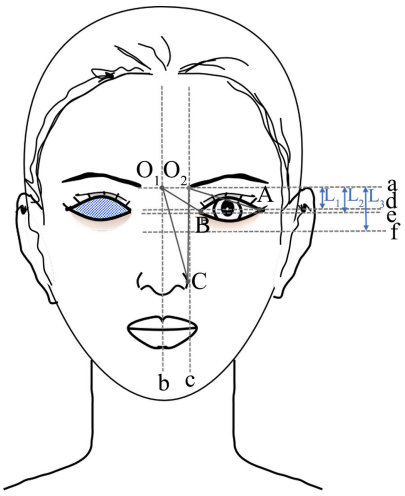

Figure 1. Definition of geometric parameters for quantitative analysis of periocular morphology. This schematic defines the landmarks and reference lines used to assess eye-area morphology. Key points include: A, outer canthus; B, inner canthus; C, alar base; O_1, glabella; O_2, eyebrow medial end. Reference lines: a - f are horizontal or vertical lines through these points. Measured parameters include: L_1 - L_3: vertical distances from line a to lines d, e, and f, reflecting outer canthus elevation, inner canthus elevation, and lower eyelid tightening, respectively (smaller values indicate better lifting/tightening). Angle A ($\angle AO_2C$) and Angle B ($\angle BO_1C$): lateral and medial eye-opening angles; larger values reflect greater lifting. Palpebral fissure area: the gap between upper and lower eyelids; larger area indicates improved eye-opening effect.

All parameters, except geometric measurements (baseline and day 28 only), were assessed bilaterally at all timepoints. Data were analyzed and expressed as mean ± SD. Normally distributed variables were compared with paired t-tests, while non-normally distributed variables were analyzed with Wilcoxon signed-rank tests, with significance set at $\alpha = 0.05$.

3. Results

3.1. PDRN Demonstrates High Biocompatibility and Dose Selection Rationale

To assess the cytotoxicity of PDRN and establish suitable concentrations for subsequent experiments, an MTT assay was performed on HDFs treated with 0.1 - 100 μg/mL PDRN for 48 h. As shown in Figure 2, PDRN exhibited no significant cytotoxicity, with cell viability remaining at 93.90% even at the highest concentration tested. These findings demonstrate that PDRN is well tolerated and highly biocompatible with dermal fibroblasts.

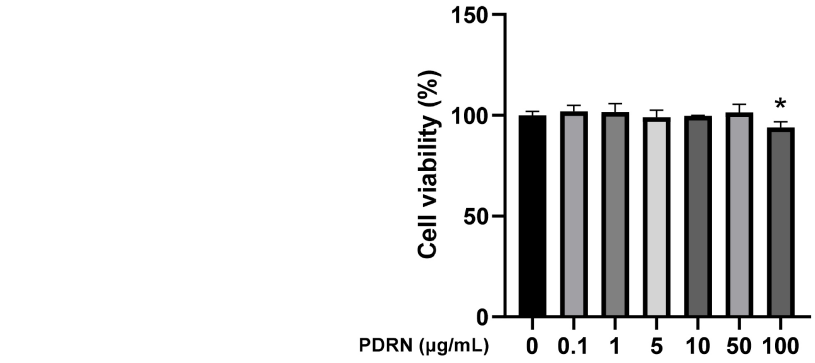

Figure 2. Cell viability assay results of PDRN on human dermal fibroblasts (n = 3, mean ± SEM, *: compared with control, $p < 0.05$).

Based on the safety profile and pharmacological rationale, 0.1 μg/mL and 0.25 μg/mL were selected for subsequent experiments. These lower concentrations were chosen not only for their tolerability but also for biological relevance, as PDRN, a macromolecular DNA derivative, is thought to act primarily through cell surface receptor activation (e.g., A2A receptors) and endocytic uptake. Under such mechanisms, lower concentrations are often more effective due to receptor sensitivity and the potential for optimized signal transduction.

3.2. PDRN Restores Key ECM Proteins in UV-Irradiated Human Dermal Fibroblasts

To assess the regenerative potential of PDRN in photoaged skin, we examined ECM protein expression in UVB-irradiated HDFs following PDRN treatment. Immunofluorescence staining revealed that PDRN significantly increased the expression of collagen I, collagen III, and elastin in a dose-dependent manner (Figure 3).

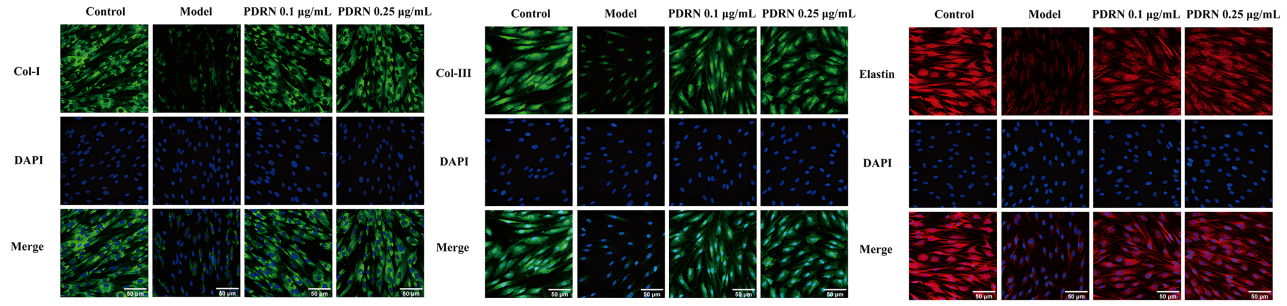

Figure 3. Immunofluorescence staining results of PDRN on the expression of collagen I (Col-I), collagen III (Col-III), and elastin.

Specifically, treatment with 0.1 μg/mL and 0.25 μg/mL PDRN for 48 h increased collagen I expression by 299.64% and 312.82%, respectively, compared with the UVB-only group ($p < 0.001$, one-way ANOVA). Collagen III levels rose by 470.32% and 564.18%, while elastin expression increased by 231.12% and 256.54% at the same concentrations ($p < 0.001$). As summarized in **Figure 4**, these results demonstrate that PDRN effectively counteracts UV-induced ECM protein loss in dermal fibroblasts.

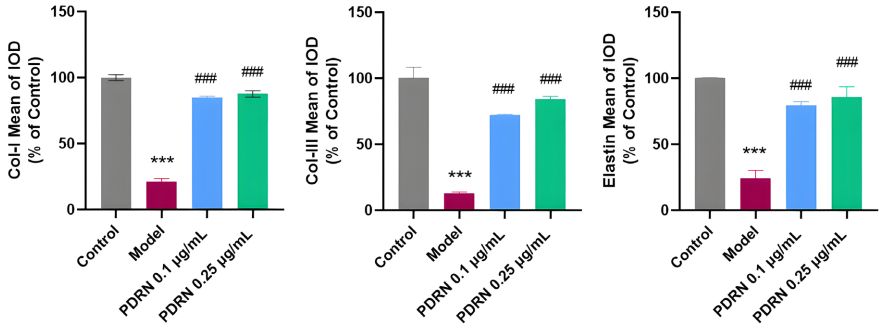

Figure 4. PDRN restores ECM protein expression in UV-damaged human dermal fibroblasts (n = 3, mean ± SEM, ***: compared with control, $p < 0.001$, ###: compared with model, $p < 0.001$).

3.3. Transcriptomic Profiling Reveals Multi-Pathway Mechanisms Underlying PDRN-Induced Rejuvenation

To elucidate the molecular mechanisms underlying PDRN's regenerative effects on UV-damaged fibroblasts, transcriptomic profiling was performed using RNA sequencing. Principal component analysis (PCA) and sample correlation analysis demonstrated clear separation between UVB-damaged (Model) and PDRN-treated groups, confirming high data quality and biological reproducibility (**Figure 5**).

Differential expression analysis revealed broad and coordinated changes in gene expression following PDRN treatment. Genes associated with the PI3K-Akt signaling pathway, including BCL3, PIK3CG, and FOXC1, were significantly upregulated (**Figure 6**), indicating enhanced cell survival signaling. Gene Ontology (GO) and Gene Set Enrichment Analysis (GSEA) further showed suppression of apoptosis- and necroptosis-related pathways, consistent with the viability data

from the MTT assay and suggesting that PDRN enables UV-stressed fibroblasts to resist programmed cell death.

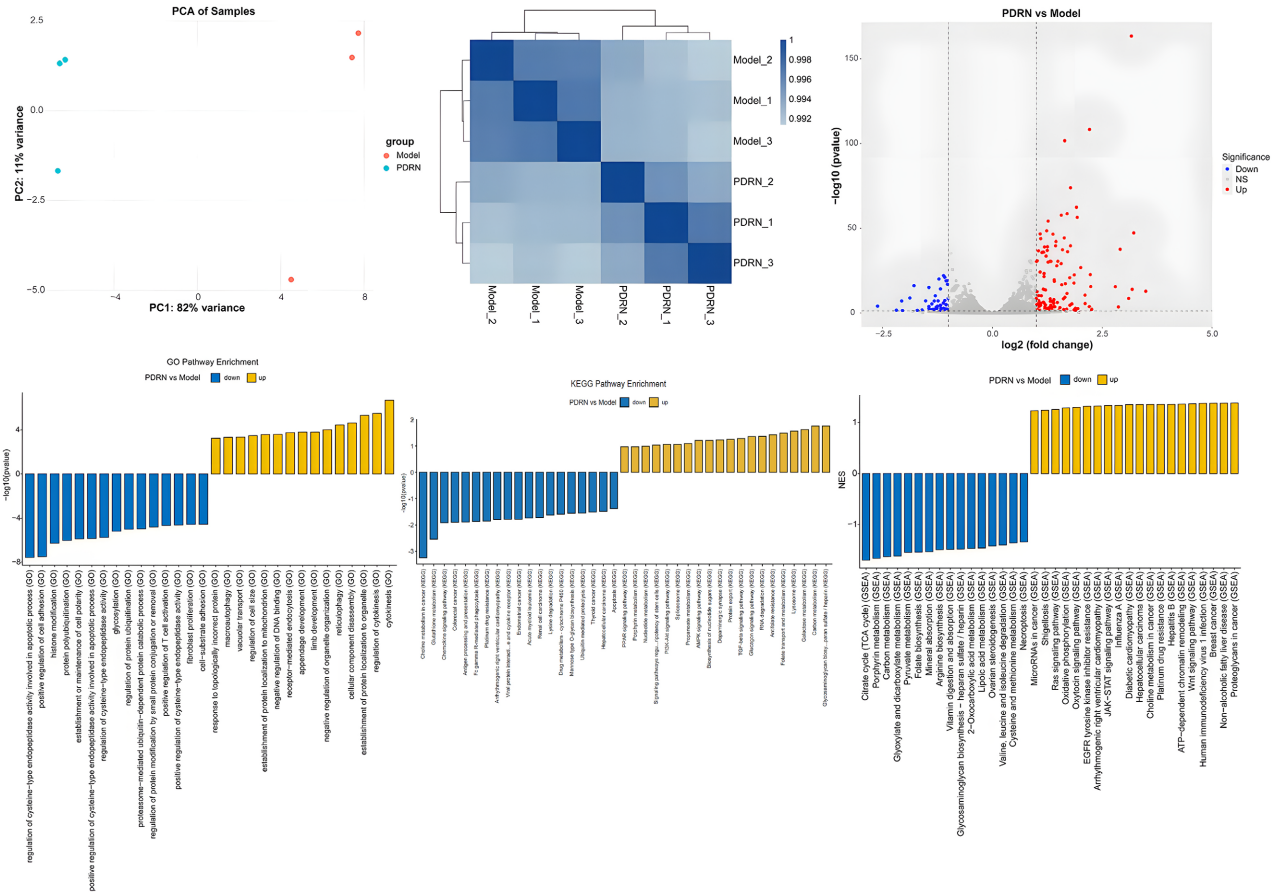

Figure 5. Transcriptomic profiling reveals multi-pathway regenerative effects of PDRN in UVB-damaged human dermal fibroblasts.

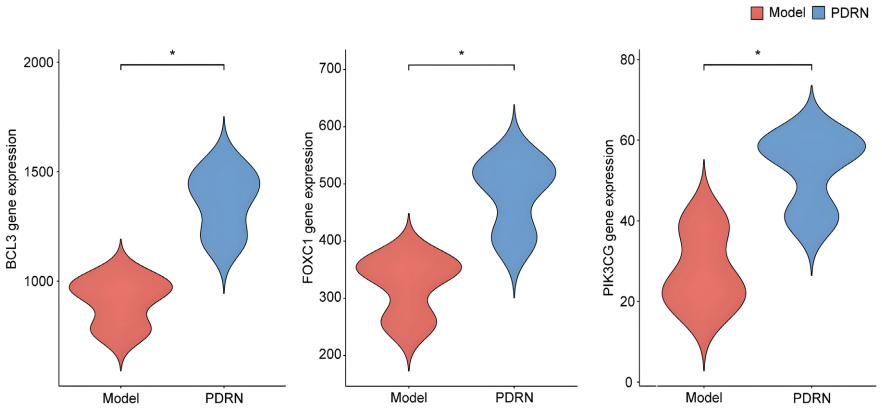

Figure 6. PDRN activates genes involved in PI3K-Akt signaling to promote fibroblast survival in UVB-damaged human dermal fibroblasts (*: compared with model, $p < 0.05$).

In parallel, PDRN stimulated ECM regeneration. Key regulators of the TGF-*β*/SMAD pathway, such as SMAD3 and TGFBI, were upregulated (**Figure 7**), accompanied by increased expression of matrix components including COL16A1

and ELN, as well as enrichment of glycosaminoglycan biosynthesis pathways. Concurrently, ECM-degrading enzymes such as MMP1 and MMP10 were downregulated, indicating a dual mechanism of enhanced matrix synthesis and reduced degradation that collectively supports ECM restoration.

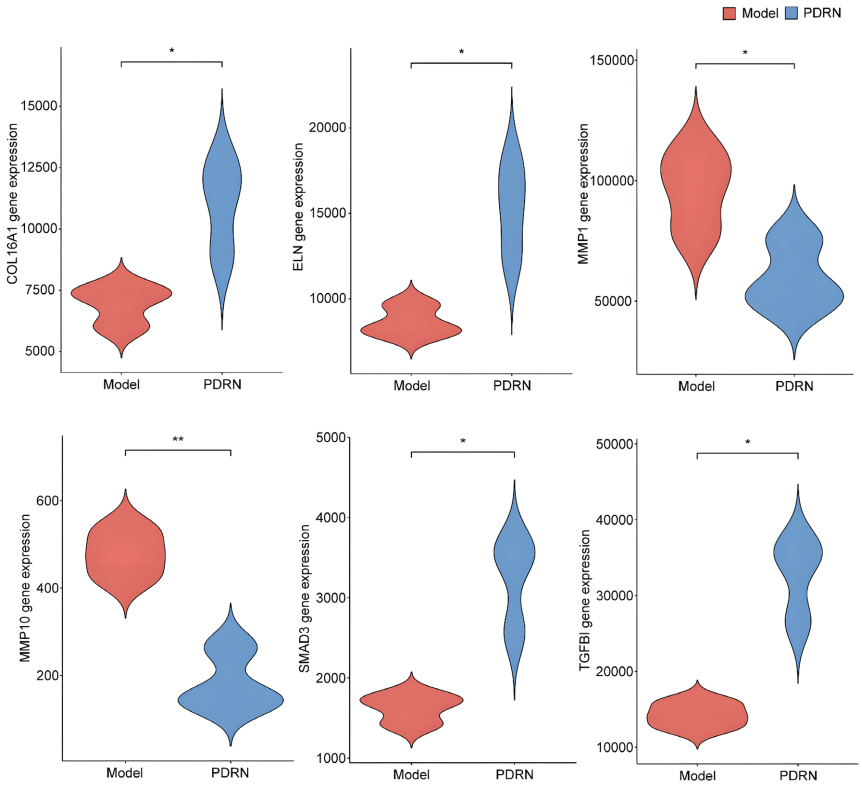

Figure 7. PDRN modulates key gene expression involved in extracellular matrix remodeling and TGF-β/SMAD signaling in UV-irradiated human dermal fibroblasts (*: compared with model, $p < 0.05$).

Transcriptomic data also highlighted activation of proliferative and reparative signaling cascades. Genes involved in Wnt and JAK-STAT pathways were enriched in PDRN-treated fibroblasts, underscoring its role in promoting fibroblast regeneration and phenotypic recovery. Pathways regulating proteostasis and autophagy were notably altered: PDRN upregulated genes associated with macroautophagy, reticulophagy, and lysosomal degradation, thereby enhancing the clearance of damaged organelles and maintaining intracellular homeostasis. In contrast, genes of the ubiquitin-proteasome system were downregulated, potentially reflecting a reduced burden of damaged proteins or stabilization of essential proteins under improved cellular conditions. Upregulation of spliceosome pathway genes further suggested improved fidelity of mRNA processing and protein synthesis.

Finally, PDRN exerted anti-inflammatory effects at the transcriptomic level. Chemokine-related genes and inflammatory mediators were broadly suppressed, with KEGG pathway analysis confirming significant downregulation of chemo-

kine signaling pathways. This transcriptomic signature indicates that PDRN contributes to a regenerative microenvironment by simultaneously dampening inflammation and supporting tissue repair.

Taken together, the RNA-seq data demonstrate that PDRN orchestrates a multifaceted regenerative program in UV-damaged dermal fibroblasts. By concurrently enhancing cell survival, stimulating ECM synthesis, modulating proliferative and homeostatic pathways, and suppressing inflammatory signaling, PDRN activates multiple molecular mechanisms that collectively facilitate dermal repair and counteract photoaging (Figure 8).

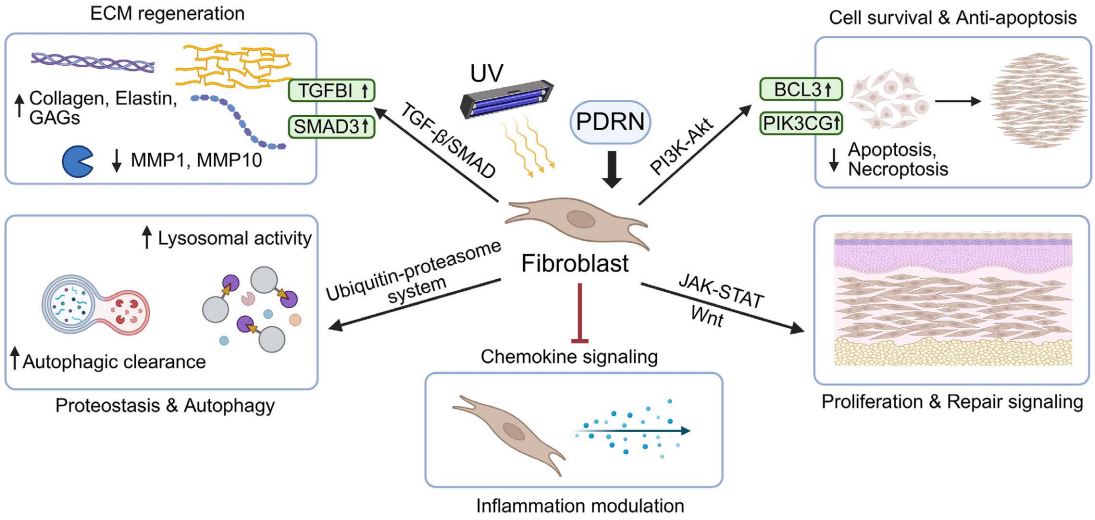

Figure 8. Schematic summary of the anti-photoaging mechanisms of PDRN in UV-damaged human dermal fibroblasts.

3.4. *Ex Vivo* Skin Penetration Study Reveals Time-Dependent PDRN Delivery into the Epidermis and Dermis

Raman spectroscopy was employed to evaluate the *ex vivo* penetration of PDRN into human skin, with the characteristic Raman peak at 1081 cm^{-1} used as a molecular marker. Compared with blank controls, PDRN-treated samples showed significantly higher total integrated intensities in both the epidermis and dermis at 2, 6, and 24 h (all $p < 0.01$), confirming measurable transcutaneous delivery (Figure 9).

In whole-skin analysis, total integrated intensity increased from 558.46 ± 135.25 a.u. at 2 h to 760.89 ± 44.73 a.u. at 6 h, and further to 1037.77 ± 37.26 a.u. at 24 h, representing a 36.39% rise between 6 and 24 h. Layer-specific analysis revealed epidermal intensities of 320.65 ± 8.84 a.u. at 2 h, 407.87 ± 4.08 a.u. at 6 h, and 430.75 ± 4.87 a.u. at 24 h. In the dermis, penetration increased from 237.81 ± 126.49 a.u. at 2 h to 353.02 ± 45.18 a.u. at 6 h, reaching 607.01 ± 32.39 a.u. at 24 h—a 71.95% increase between 6 and 24 h.

Depth profiling further demonstrated progressive penetration, with depths of 43.33 ± 2.89 μm at 2 h, 121.67 ± 2.89 μm at 6 h, and 233.33 ± 7.64 μm at 24 h, confirming time-dependent diffusion of PDRN across the skin barrier.

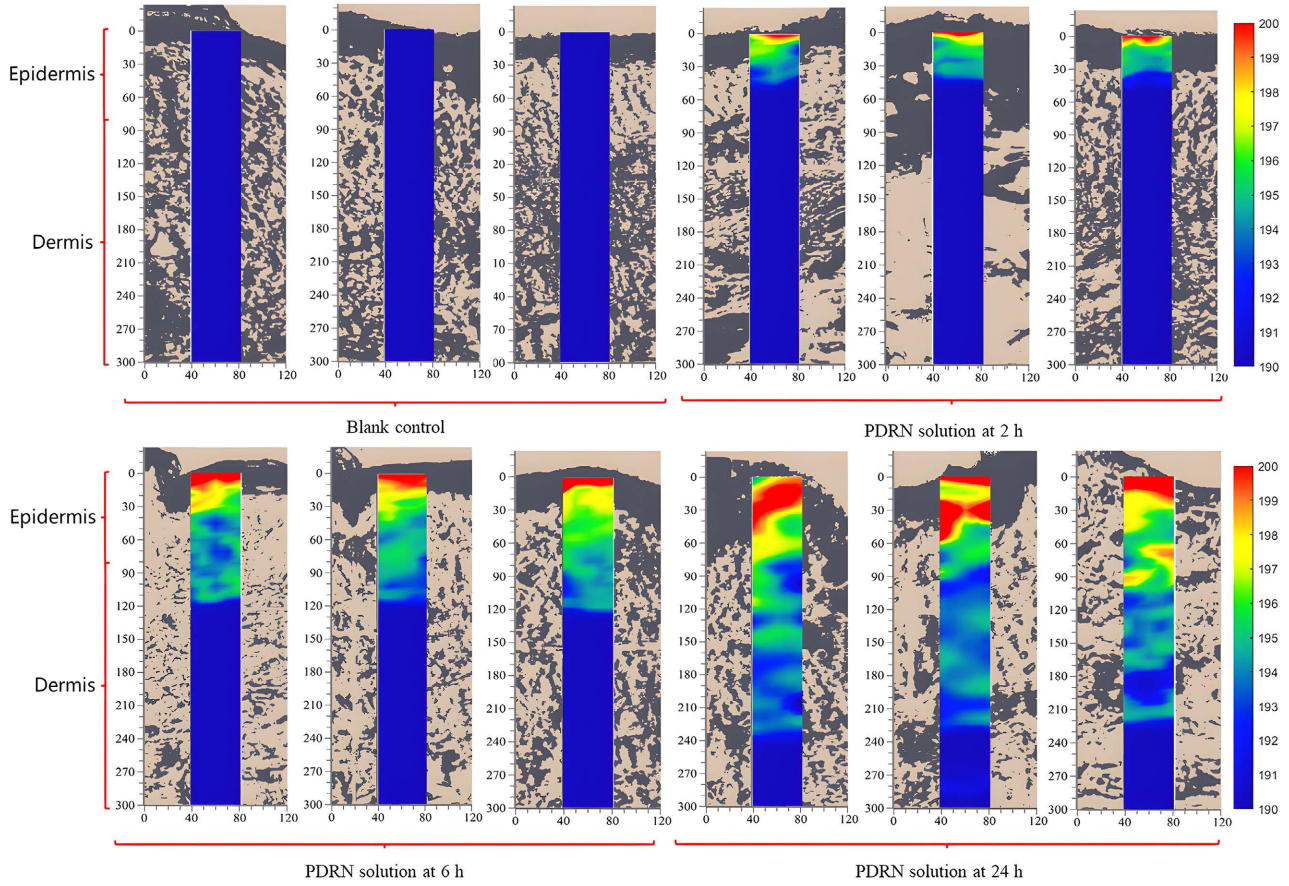

Figure 9. *Ex vivo* skin penetration of PDRN visualized by Raman spectroscopy.

3.5. PDRN Eye Cream Significantly Improves Periocular Elasticity, Dermal Density, Wrinkles, Puffiness, and Contour after 28 Days

A self-controlled clinical trial was conducted to evaluate the anti-aging efficacy of a PDRN-containing eye cream after 28 days of use. Multidimensional assessments of periocular skin parameters showed that, compared with baseline, PDRN treatment significantly improved skin elasticity (R2, R5, R7) and firmness (R0, F4) in 33 subjects, with changes markedly greater than those in the placebo group ($p < 0.05$), indicating enhanced biomechanical properties of periocular skin.

After 28 days, dermal density increased by 8.67%, accompanied by significant reductions in the number and area of crow's feet, under-eye wrinkles, and tear-trough wrinkles, as well as wrinkle volume and periorbital skin roughness (all $p < 0.05$ vs. placebo), suggesting that PDRN promotes dermal repair and reduces wrinkle severity. Specifically, crow's feet number and area improved by 12.06% and 10.31%, under-eye wrinkle number and area by 27.06% and 10.38%, tear-trough wrinkle length and volume by 16.37% and 18.11%, and canthal skin roughness by 9.27%. Furthermore, under-eye bag volume decreased by 18.42%, while skin lightness (L) increased by 4.88%, both significantly superior to placebo, reflecting improvements in under-eye puffiness and skin radiance.

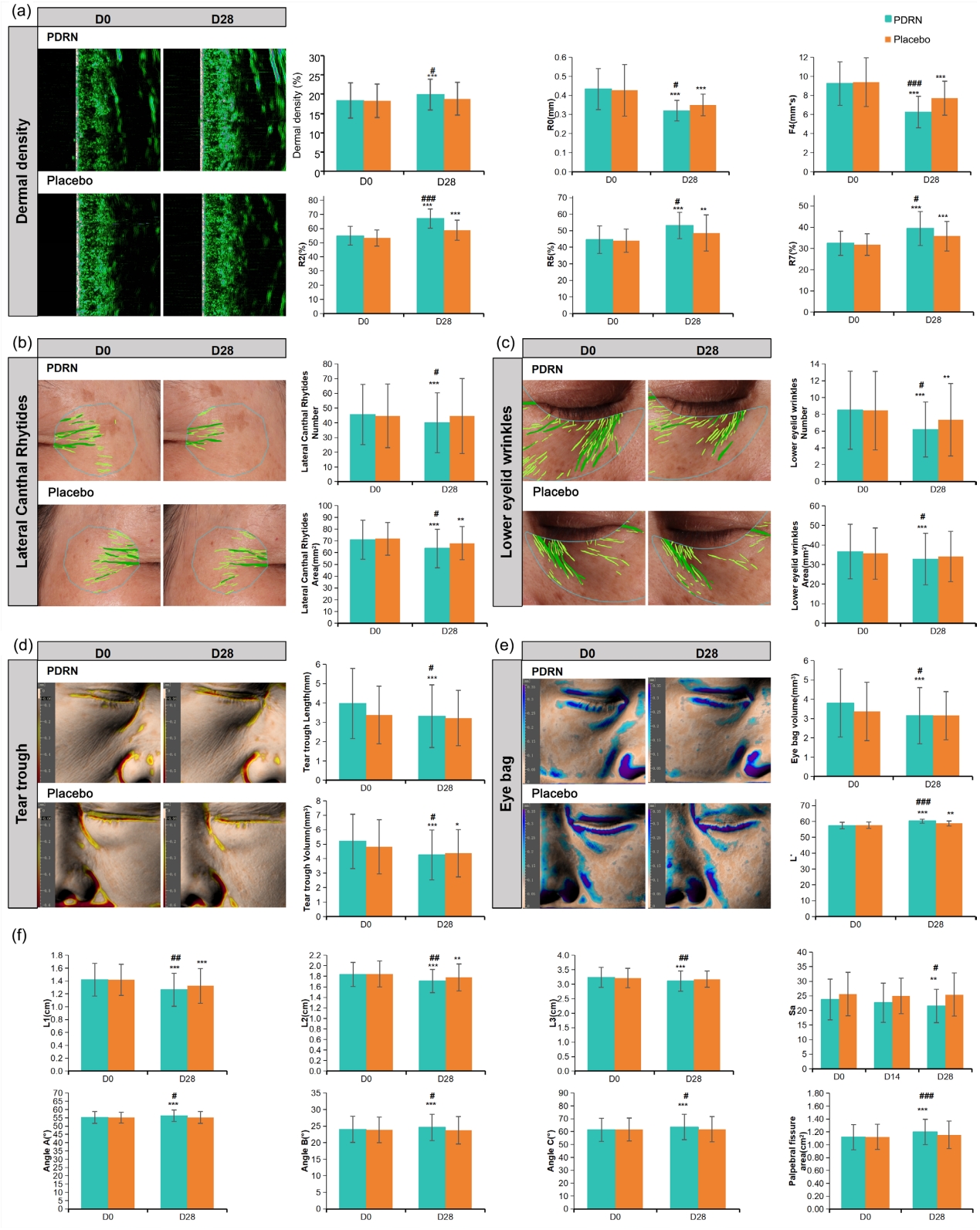

Figure 10. Clinical Efficacy Comparison between PDRN Eye Cream and Placebo Cream. (a) Dermal density and elasticity/firmness; (b) Crow's feet; (c) Under-eye wrinkles; (d) Tear-trough wrinkles; (e) Eye bag volume and skin lightness (L value); (f) Periocular linear angles and canthal skin roughness. Data are shown as mean ± SD (n = 33). $p < 0.05$, $p < 0.01$, $p < 0.001$ vs. baseline; #$p < 0.05$, ##$p < 0.01$, ###$p < 0.001$ vs. Placebo.

Morphological analyses revealed significantly greater improvements on the PDRN-treated side compared with placebo. Eye distance L1 and angle A (outer canthus) improved by 11.27% and 1.76%, respectively; eye distance L2 and angle B (inner canthus) improved by 7.07% and 2.37%; and parameters associated with eyelid tightness—eye distance L3, eye area, and upper–lower eyelid angle C—improved by 3.72%, 7.14%, and 3.55%, respectively. These findings indicate that PDRN optimizes periocular angles and contours.

Taken together, the PDRN-containing eye cream demonstrated significantly greater efficacy than placebo in improving periocular elasticity, dermal density, wrinkle appearance, under-eye puffiness, brightness, and contour definition (**Figure 10**), thereby enhancing both the appearance and structural condition of periocular skin.

4. Discussion

This study provides novel insights into the anti-aging potential of PDRN, demonstrating that it acts through multi-pathway modulation of fibroblast activity. Beyond its well-documented role in promoting ECM synthesis, our transcriptomic and functional findings show that PDRN influences a broader network of cellular processes—including cell survival, ECM remodeling, proteostasis, and inflammatory signaling—positioning it as a comprehensive modulator of dermal homeostasis.

A central mechanistic observation is the concurrent activation of PI3K–Akt and TGF-β/SMAD signaling pathways. PI3K–Akt is a master regulator of fibroblast survival, proliferation, and biosynthetic capacity [19], while TGF-β is the canonical driver of collagen and elastin synthesis [20]. The combined enhancement of these pathways provides a strong explanation for the robust restoration of type I/III collagen and elastin observed in UVB-damaged fibroblasts. Our RNA-seq data reveal these pathways as key nodes in PDRN's activity; future studies employing functional validation, such as inhibitor assays or receptor-level interrogation, will be critical to confirm causality and further delineate upstream drivers.

The known pharmacology of PDRN as an adenosine A2A receptor agonist provides a compelling mechanistic link. Activation of A2A receptors has been shown to stimulate PI3K-Akt signaling [21], while also interacting with TGF-β/SMAD networks [22], thereby supporting both fibroblast survival and ECM synthesis. Although receptor engagement was not directly tested in this study, these established pathways offer a biologically plausible explanation for the transcriptomic changes we observed and highlight a clear direction for future mechanistic work.

Beyond canonical pathways, PDRN also influenced proteostasis and autophagy, processes increasingly recognized as hallmarks of skin aging [23]. Upregulation of lysosomal and autophagy-related genes, together with downregulation of ubiquitin-proteasome components, suggests a shift toward enhanced clearance of damaged proteins and organelles. Upregulation of spliceosome-related pathways further indicates potential improvements in mRNA processing and protein synthesis fidelity. While these observations provide intriguing leads, they remain

transcriptomic signatures; follow-up studies using functional assays, autophagosome imaging, or splicing efficiency metrics will be valuable to confirm these effects and establish their contribution to PDRN's anti-aging action.

PDRN also exerted immunomodulatory effects. UV irradiation activates pro-inflammatory cascades, including CCL8-CCR and IL-17 signaling, which promote fibroblast stress, pigmentation, and ECM breakdown [24] [25]. PDRN attenuated these inflammatory signatures, with transcriptomic analysis indicating downregulation of chemokine-related pathways. Although individual chemokine transcripts were not directly measured in this study, prior evidence suggests that genes such as CCL2 and CXCL5 may be involved [26] [27]. These candidates will require gene-specific validation in future experiments. Moreover, as our in vitro model was fibroblast-centric, it did not capture the full complexity of fibroblast - immune crosstalk. Co-culture systems, 3D skin equivalents, or in vivo models will be necessary to determine whether PDRN truly rebalances fibroblast - immune interactions in the full skin microenvironment.

From a methodological perspective, Raman spectroscopy confirmed that PDRN, despite being a macromolecule, penetrates into the dermis. It is important to note, however, that Raman spectroscopy provides semi-quantitative data (integrated intensity) rather than absolute concentrations, as signal strength is influenced by tissue scattering and hydration state. Thus, while our study establishes proof-of-principle of dermal delivery, pharmacokinetic studies using complementary approaches (e.g., radiolabeling or mass spectrometry) will be required to determine absolute tissue concentrations.

The clinical outcomes—enhanced elasticity, increased dermal density, wrinkle reduction, and decreased puffiness, align with the mechanistic signatures observed: PI3K-Akt-driven survival, TGF-β-mediated ECM restoration, and suppression of inflammation. We also acknowledge that placebo effects were evident, as the placebo cream was formulated to provide hydration and barrier support. Such moisturization is known to transiently improve elasticity and surface smoothness. However, the superior outcomes with the PDRN cream, particularly in dermal density, wrinkle reduction, and contour geometry, indicate that the observed benefits extend beyond hydration alone. The periocular area is among the most delicate regions of the face, with thin skin, limited structural protein reserves, and high mobility, making it especially prone to wrinkles, laxity, puffiness, and pigmentation. Because multiple biological processes contribute simultaneously to periocular aging, interventions that act on a single pathway often yield incomplete results. PDRN's ability to engage multiple pathways in parallel makes it particularly well-suited to address the complex and multifactorial nature of periocular aging.

Several additional limitations should be highlighted. First, we did not include a non-UVB + PDRN group in our in vitro design, which would have clarified whether PDRN exerts benefits beyond restoring UV-induced damage. Second, the clinical trial was limited to 28 days in an Asian female cohort, leaving open questions of durability, rebound effects, and generalizability across ethnicities and sexes.

Third, our study did not address alternative explanations for PDRN's effects, such as its role as a purine source via the salvage pathway, which may complement receptor-mediated signaling [15]. Looking forward, future studies should include comprehensive dose - response analyses of ECM protein expression to refine the effective range identified here (0.1 - 0.25 μg/mL) which may be more effective for receptor-mediated activities and endocytosis, alongside functional validation of autophagy and spliceosome pathways, and co-culture or 3D models to assess immune crosstalk. Pharmacokinetic studies are also needed to establish tissue-level concentrations, and longer-term clinical trials will be necessary to evaluate durability of effects. Comparative trials against established actives such as retinoids will be particularly informative, as retinoids are effective ECM stimulants [8].

Finally, while this study focused on the periocular area due to its thin skin, mobility, and susceptibility to multiple aging signs, the multi-pathway modulatory profile of PDRN may make it relevant for broader applications in facial and photoexposed skin. Moreover, given that PDRN is a DNA-derived biomaterial that can be manufactured at scale, future work may explore its cost-effectiveness and feasibility for wider cosmetic use.

5. Conclusions

This study establishes PDRN as a novel multifunctional topical active for skin rejuvenation. In UV-damaged fibroblasts, PDRN not only restored ECM proteins but also modulated interconnected transcriptomic networks governing cell survival, proteostasis, and inflammatory balance. *Ex vivo* Raman spectroscopy confirmed its ability to traverse the skin barrier and reach dermal targets. Clinically, a PDRN-containing eye cream produced significant improvements in elasticity, dermal density, wrinkle severity, under-eye puffiness, brightness, and periocular contour after 28 days, with outcomes superior to placebo.

Taken together, these findings provide the first integrated evidence that PDRN engages multiple pathways to restore dermal homeostasis, achieves effective dermal delivery despite its macromolecular nature, and translates into clinically meaningful improvements in periocular aging. Future work extending into longer-term trials, pharmacokinetic studies, and comparative evaluations against established actives will be instrumental in defining PDRN's place in the anti-aging armamentarium. PDRN therefore represents a promising next-generation bioactive capable of addressing the multifactorial drivers of skin aging, with potential applications that extend beyond the periocular area to broader facial and photoexposed skin.

Conflicts of Interest

The authors declare no conflicts of interest.

References

[1] Hussein, R.S., Bin Dayel, S., Abahussein, O. and El-Sherbiny, A.A. (2025) Influences on Skin and Intrinsic Aging: Biological, Environmental, and Therapeutic Insights. *Journal of Cosmetic Dermatology*, **24**, e16688. https://doi.org/10.1111/jocd.16688

[2] Shin, S.H., Lee, Y.H., Rho, N. and Park, K.Y. (2023) Skin Aging from Mechanisms to Interventions: Focusing on Dermal Aging. *Frontiers in Physiology*, **14**, Article 1195272. https://doi.org/10.3389/fphys.2023.1195272

[3] Flament, F., Bazin, R., Rubert, L.S., *et al.* (2013) Effect of the Sun on Visible Clinical Signs of Aging in Caucasian Skin. *Clinical, Cosmetic and Investigational Dermatology*, **6**, 221-232. https://doi.org/10.2147/ccid.s44686

[4] Panich, U., Sittithumcharee, G., Rathviboon, N. and Jirawatnotai, S. (2016) Ultraviolet Radiation-Induced Skin Aging: The Role of DNA Damage and Oxidative Stress in Epidermal Stem Cell Damage Mediated Skin Aging. *Stem Cells International*, **2016**, Article 7370642. https://doi.org/10.1155/2016/7370642

[5] Watson, R.E.B., Gibbs, N.K., Griffiths, C.E.M. and Sherratt, M.J. (2014) Damage to Skin Extracellular Matrix Induced by UV Exposure. *Antioxidants & Redox Signaling*, **21**, 1063-1077. https://doi.org/10.1089/ars.2013.5653

[6] Kim, D.J., Iwasaki, A., Chien, A.L. and Kang, S. (2022) UVB-Mediated DNA Damage Induces Matrix Metalloproteinases to Promote Photoaging in an AhR and SP1-Dependent Manner. *JCI Insight*, **7**, e156344. https://doi.org/10.1172/jci.insight.156344

[7] Shin, J., Kwon, S., Choi, J., Na, J., Huh, C., Choi, H., *et al.* (2019) Molecular Mechanisms of Dermal Aging and Antiaging Approaches. *International Journal of Molecular Sciences*, **20**, Article 2126. https://doi.org/10.3390/ijms20092126

[8] Wang, Q., Hu, F., Hu, X., Xie, Y., Du, L. and Ye, R. (2023) The Synergistic Effect of Retinyl Propionate and Hydroxypinacolone Retinoate on Skin Aging. *Journal of Cosmetic Dermatology*, **22**, 2040-2049. https://doi.org/10.1111/jocd.15662

[9] Al-Niaimi, F. and Chiang, N.Y.Z. (2017) Topical Vitamin C and the Skin: Mechanisms of Action and Clinical Applications. *Journal of Clinical and Aesthetic Dermatology*, **10**, 14-17.

[10] Maia Campos, P.M.B.G., Melo, M.O. and Siqueira César, F.C. (2019) Topical Application and Oral Supplementation of Peptides in the Improvement of Skin Viscoelasticity and Density. *Journal of Cosmetic Dermatology*, **18**, 1693-1699. https://doi.org/10.1111/jocd.12893

[11] Wang, Q., Zhong, Y., Li, N., Du, L., Ye, R., Xie, Y., *et al.* (2023) Combination of Dimethylmethoxy Chromanol and Turmeric Root Extract Synergically Attenuates Ultraviolet-Induced Oxidative Damage by Increasing Endogenous Antioxidants in Hacat Cells. *Skin Research and Technology*, **29**, e13539. https://doi.org/10.1111/srt.13539

[12] Leok Goh, C., Tang, M.B.Y., Briantais, P., Kaoukhov, A. and Soto, P. (2009) Adapalene Gel 0.1% Is Better Tolerated than Tretinoin Gel 0.025% among Healthy Volunteers of Various Ethnic Origins. *Journal of Dermatological Treatment*, **20**, 282-288. https://doi.org/10.1080/09546630902763164

[13] Bai, D., Hu, F., Xu, H., Huang, J., Wu, C., Zhang, J., *et al.* (2023) High Stability and Low Irritation of Retinol Propionate and Hydroxypinacolone Retinoate Supramolecular Nanoparticles with Effective Anti-Wrinkle Efficacy. *Pharmaceutics*, **15**, Article 731. https://doi.org/10.3390/pharmaceutics15030731

[14] Veronesi, F., Dallari, D., Sabbioni, G., Carubbi, C., Martini, L. and Fini, M. (2017) Polydeoxyribonucleotides (PDRNs) from Skin to Musculoskeletal Tissue Regeneration via Adenosine A2A Receptor Involvement. *Journal of Cellular Physiology*, **232**, 2299-2307. https://doi.org/10.1002/jcp.25663

[15] Squadrito, F., Bitto, A., Irrera, N., Pizzino, G., Pallio, G., Minutoli, L., *et al.* (2017) Pharmacological Activity and Clinical Use of PDRN. *Frontiers in Pharmacology*, **8**, Article 224. https://doi.org/10.3389/fphar.2017.00224

[16] Marques, C., Porcello, A., Cerrano, M., Hadjab, F., Chemali, M., Lourenço, K., *et al.* (2025) From Polydeoxyribonucleotides (PDRNs) to Polynucleotides (PNs): Bridging the Gap between Scientific Definitions, Molecular Insights, and Clinical Applications of Multifunctional Biomolecules. *Biomolecules*, **15**, Article 148 https://doi.org/10.3390/biom15010148

[17] Hwang, K.H., Kim, J.H., Park, E.Y. and Cha, S.K. (2018) An Effective Range of Polydeoxyribonucleotides Is Critical for Wound Healing Quality. *Molecular Medicine Reports*, **18**, 5166-5172. https://doi.org/10.3892/mmr.2018.9539

[18] Alkilani, A.Z., McCrudden, M.T. and Donnelly, R.F. (2015) Transdermal Drug Delivery: Innovative Pharmaceutical Developments Based on Disruption of the Barrier Properties of the Stratum Corneum. *Pharmaceutics*, **7**, 438-470. https://doi.org/10.3390/pharmaceutics7040438

[19] Pal, I. and Mandal, M. (2012) PI3K and Akt as Molecular Targets for Cancer Therapy: Current Clinical Outcomes. *Acta Pharmacologica Sinica*, **33**, 1441-1458. https://doi.org/10.1038/aps.2012.72

[20] Ke, Y. and Wang, X. (2021) TGFβ Signaling in Photoaging and UV-Induced Skin Cancer. *Journal of Investigative Dermatology*, **141**, 1104-1110. https://doi.org/10.1016/j.jid.2020.11.007

[21] Shi, L., Wu, Z., Miao, J., Du, S., Ai, S., Xu, E., *et al.* (2019) Adenosine Interaction with Adenosine Receptor A2A Promotes Gastric Cancer Metastasis by Enhancing PI3K-Akt-mTOR Signaling. *Molecular Biology of the Cell*, **30**, 2527-2534. https://doi.org/10.1091/mbc.e19-03-0136

[22] Zhang, Y.E. (2009) Non-Smad Pathways in TGF-β Signaling. *Cell Research*, **19**, 128-139. https://doi.org/10.1038/cr.2008.328

[23] López-Otín, C., Blasco, M.A., Partridge, L., Serrano, M. and Kroemer, G. (2023) Hallmarks of Aging: An Expanding Universe. *Cell*, **186**, 243-278. https://doi.org/10.1016/j.cell.2022.11.001

[24] Xie, Y., Yang, A., Li, N., Zheng, H., Zhong, Y., Jin, Y., *et al.* (2024) Lapagyl Mitigates UV-Induced Inflammation and Immunosuppression via Foxp3+ Tregs and CCL Pathway: A Single-Cell Transcriptomics Study. *Phytomedicine*, **129**, Article 155679. https://doi.org/10.1016/j.phymed.2024.155679

[25] Solá, P., Mereu, E., Bonjoch, J., Casado-Peláez, M., Prats, N., Aguilera, M., *et al.* (2023) Targeting Lymphoid-Derived IL-17 Signaling to Delay Skin Aging. *Nature Aging*, **3**, 688-704. https://doi.org/10.1038/s43587-023-00431-z

[26] Lee, W.J., Jo, S.Y., Lee, M.H., Won, C.H., *et al.* (2016) The Effect of MCP-1/CCR2 on the Proliferation and Senescence of Epidermal Constituent Cells in Solar Lentigo. *International Journal of Molecular Sciences*, **17**, Article 948. https://doi.org/10.3390/ijms17060948

[27] Reichert, O., Kolbe, L., Terstegen, L., Staeb, F., Wenck, H., Schmelz, M., *et al.* (2015) UV Radiation Induces CXCL5 Expression in Human Skin. *Experimental Dermatology*, **24**, 309-312. https://doi.org/10.1111/exd.12652